

A pilot spectroscopy study on time-varying bioimpedance during electrically-induced muscle contraction

Benjamin Sanchez¹, Jia Li¹, Tom Geisbush¹, Ramon Bragos² and Seward B. Rutkove¹

Abstract—Alterations in the health of muscles can be evaluated through the use of electrical impedance myography (EIM). To date, however, nearly all work has relied upon single-frequency/spectroscopy stepped-sine measurements of static muscle (contracted or relaxed). In this work, we assessed the temporal alterations in the impedance spectrum (1 kHz to 1 MHz) behavior of gastrocnemius during the active process of muscle contraction. The approach is based on the multisine impedance spectroscopy technique. The gastrocnemii of a wild type mouse was measured during electrically-induced muscle contraction via direct current stimulation of the sciatic nerve. The processes of contraction and relaxation were clearly identified in the time-frequency impedance spectrum likely corresponding to an increase muscle fiber diameter. The technique of dynamic multisine EIM has the potential of providing useful insights into contractile mechanisms of muscle in health and disease.

I. INTRODUCTION

The major source of disability of most diseases that affect the peripheral nervous system and muscle is weakness. Many of these disorders, which include conditions such as amyotrophic lateral sclerosis, muscular dystrophy, inflammatory myopathies, and certain polyneuropathies, are without effective therapy [1]. Fortunately, thanks to an improved understanding into the pathogenesis of these diseases and creative new therapeutic strategies, new discoveries are beginning to yield concrete advances and certain diseases, previously thought to be untreatable, such as Duchenne muscular dystrophy, are now finding potential effective therapy [2]. Still, a great deal of work needs to be accomplished if the weakness produced by these diseases is to be effectively ameliorated.

Electrical impedance myography (EIM) [3] is a non-invasive tool to evaluate the structural and functional properties of muscle and it has shown to be sensitive to the presence and severity of neuromuscular disorders [4], for example, to monitor disease status and effects of therapy in amyotrophic lateral sclerosis [5]. The working principle of EIM is based on a tetrapolar impedance measurement technique in which localized measurements of muscle are made and the electrical

impedance, i.e. reactance and resistance, are used to assess muscle health. Classical EIM approaches have relied on the measurement of the muscle impedance spectrum at a single-frequency frequency of electrical current applied. To date, nearly all EIM work has been focused on static, relaxed muscle.

However, we have remarkably little insight into how these structural alterations impact the dynamic behavior of the myocyte during the contractile process itself both over the short and long term. With the advent a variety of new potential therapeutics the ability to assess the response of the tissue to therapy is becoming increasingly important. And yet we are only able to do so at the molecular level or at the level of the entire organ, the latter by measuring force or power exerted by the muscle during the contraction. EIM spectroscopy measurements to assess contractile function at the mesoscale—i.e. intermediate in size between the molecule and the entire muscle—would provide valuable insights both into disease mechanisms and for monitoring drug effect in both animals and humans.

Thus, here we introduce a *full-spectroscopy* approach for dynamic-EIM, the underlying hypothesis of which is that electrically-induced muscle contraction produce distinct alterations in the mesoscale behavior of muscle as already observed at a single frequency [6] and that these alterations can be detected and quantified using multisine impedance spectroscopy technique.

II. IMPEDANCE INSTRUMENTATION

Regarding the techniques applied to EIM measurements, most have been based on classical digital/analogue stepped-sine based impedance analyzers [7], e.g. based on the auto-balancing bridge like the HP4192 from Hewlett-Packard. However, the measuring instrument that has revolutionized the spectroscopy measurements over the past decades is the frequency response analyzer (FRA), e.g. 1296 from Solartron Analytical. The impedance spectrum is determined by correlating, at each frequency, the response with a phase and quadrature signals and integrating (Figure 1) [8].

Despite being a relatively simple and effective method, the phase/quadrature-demodulator technique is limited when full-spectroscopy measurements are required in a short time. To illustrate this, one can see in Figure 2 an example to monitor the muscle dynamic impedance changes during contraction. In the stepped-sine approach (A), the muscle nerve would need to be stimulated many times as long as it takes to the impedancemeter to acquire a complete spectrum. Aside from the fact that it is necessary to stimulate the nerve

*This work was supported by Redes de Investigación del Instituto Carlos III (REDINSCOR, RD06/0003) and Fondo Europeo de Desarrollo Regional (FEDER), and in part by grant R01NS055099 to the Beth Israel Deaconess Medical Center General Clinical Research Center from the National Institute of Health.

¹B. Sanchez, J. Li, T. Geisbush and S. B. Rutkove are with Department of Neurology, Division of Neuromuscular Diseases, Beth Israel Deaconess Medical Center, 330 Brookline Avenue, Harvard Medical School, Boston, MA 02215-5491, USA. bsanchez@bidmc.harvard.edu

²R. Bragos is with the Electronic and Biomedical Instrumentation Group, Department of Electronic Engineering, Universitat Politècnica de Catalunya (UPC), 08034, Barcelona, Spain.

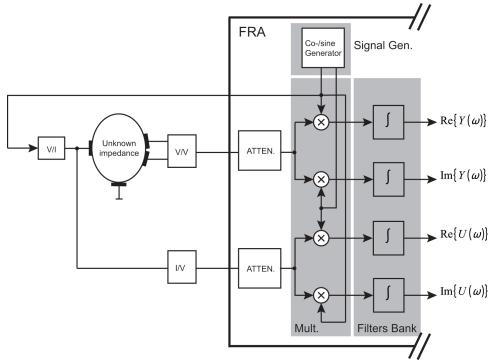


Fig. 1. Block diagram of the phase/quadrature demodulator structure of a frequency response analyzer (FRA). The estimated impedance frequency response $\hat{Z}(\omega)$ is derived from the real and imaginary parts of the input-output signals, $U(\omega)$ and $Y(\omega)$ respectively.

multiple times, one runs the risk that the first frequency measurement might be in very different muscle conditions to the last frequency measured.

However, recent digital signal processing advances [9] have opened up a new era for multifrequency FRA impedance instrumentation based on the discrete Fourier transform (DFT), e.g. based on multisines signals [10], [11], [12]. Using the multifrequency approach, many frequencies are applied simultaneously (B) and the time to acquire a complete EIM spectrum is drastically reduced making it possible to measure the instantaneous impedance changes and temporal evolution of dynamic EIM, for example, during muscle contraction and relaxation and to collect both non- and fatigued muscle data.

III. MATERIALS AND METHODS

A. Animals

The animal experimentation protocol was approved by the Beth Israel Deaconess Medical Center Institutional Animal Care and Use Committee. The mouse measured ($n=1$) was obtained from Jackson Laboratories (Bar Harbor, Maine) were allowed to acclimate for 48 hours prior to use and fed *ad libitum*.

B. Animal set up

The animal underwent all testing under 1-2% inhaled isoflurane anesthesia delivered by nosecone, with body and muscle temperature being maintained by a heating pad. The basic technique was similar to that previously described, except that gastrocnemius rather than extensor digitorum longus was studied [13]. Briefly, the skin overlaying both left and right hind-limbs was cut with a scissors and the tissue dissected down to expose the biceps femoris muscle which was removed proximally. The calcaneal tendon was cut at its insertion point, and dissected away from the underlying fascia and soleus muscle. Animal sacrifice was performed via the use of FatalPlus at the completion of measurements.

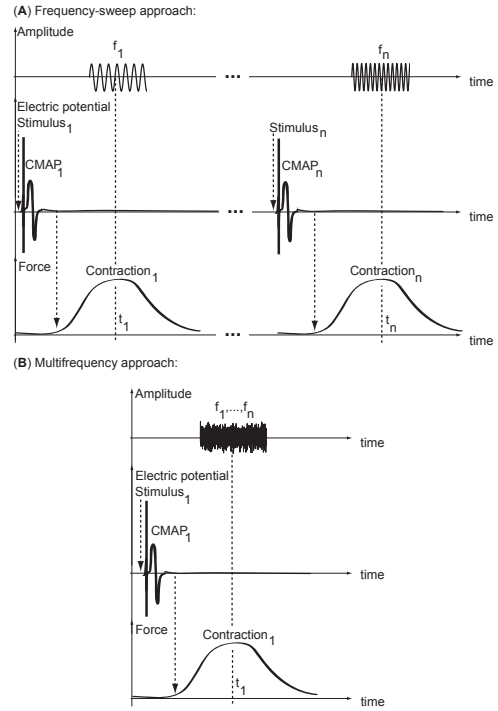


Fig. 2. Representation of the (A) stepped-sine and (B) multifrequency techniques for the measurement of dynamic EIM during muscle contraction. In (A), the muscle nerve is stimulated each time one frequency is measured while in (B) multiples frequencies are measured simultaneously with a single stimulus. Abbreviation: compound motor action potential (CMAP).

C. Nerve stimulation

To ensure that the current applied was the same for each hind leg of each animal during nerve stimulation, the compound motor action potential (CMAP) was identified first using a TECA Synergy T2 EMG Monitoring System (Viasys, Madison, WI). The CMAP was recorded via disposable ring electrodes (Product 019-435500, Faith Medical Inc., Steedman, MO) around the entire leg with stimulating the sciatic nerve at the sciatic notch (Neuroline 746 12-100/25 needle electrodes, Ambu, Denmark) [14]. The specific current which was used to obtain the CMAP was then used for the induce a moderate contraction (6 pulses at 18 Hz). By choosing these frequencies and number of stimuli, the overall duration of the contraction remained constant at 0.33 seconds.

D. Impedance measurement

The muscle impedance was measured using the custom broadband impedance frequency response analyzer (FRA) used in [11], [12]. The impedance measurement system was implemented on a rugged PC-platform PXI (PCI eXtensions for Instrumentation) platform from National Instruments. The FRA included an embedded controller PXIe-8130, a 2 channel high-speed digitizer card PXIe-5122 (100 Ms s⁻¹, 64 MB/channel, 14 bits), a 9-channel digitizer card PXI-5105 (60 Ms s⁻¹, 128 MB, 12 bits) and an Arbitrary Waveform Generator (AWG) card PXI-5422 (200 Ms s⁻¹, 32 MB, 16 bits). Synchronously to the reference excitation generated by the PXI-5422, the PXIe-5122 acquired both the noisy

$$\hat{\sigma}_{\hat{Z}}^2(k) = \left| \hat{Z}(\omega_k) \right|^2 \left(\frac{\hat{\sigma}_{\hat{V}}^2(k)}{\left| \hat{V}(k) \right|^2} + \frac{\hat{\sigma}_{\hat{I}}^2(k)}{\left| \hat{I}(k) \right|^2} - 2 \operatorname{Re} \left(\frac{\hat{\sigma}_{\hat{V}\hat{I}}^2(k)}{\hat{V}(k)\hat{I}(k)} \right) \right) \quad (2)$$

current- voltage observations coming from the analog front end (AFE) used to interface the FRA with the electrodes. The FRA analog front end consisted of a drive buffer (OPA656) and differential amplifier (AD830) for the high and the low potential terminals and a current-to-voltage converter (OPA656) for the low current sensing terminal. The details of the AFE can be found elsewhere [8].

Four disposable monopolar EMG needle electrodes of Viasys Healthcare (Ref 902-DMG50) made up the tetrapolar needle electrode array. The four strips were attached to a metal plate (30 mm L x 15 mm W) in a line with an inter-electrode separation distance of 1 mm (center to center).

For each leg, the tetrapolar electrode array was placed parallel (0 deg) to the major muscle fiber direction determined by visual inspection. The longitudinal electrode placement is the configuration for the data shown in Section IV.

E. Data acquisition and analysis

The reference excitation generated with the PXI-5422 to measure impedance was a random phase multisine signal, with $T_{\text{ms}}=1$ ms periodicity. The amplitude the harmonics were chosen to be equal (flat multisine), the phases were randomly chosen in $[0, 2\pi)$, $k \in \mathbb{K}_{\text{exc}}$ was the set of excited frequencies (26 quasi-logarithmic frequencies distributed from 1 kHz \rightarrow 939 kHz); $f_s = 5$ MHz being the sampling frequency. To avoid spectral leakage, an integer number of periods of the multisine excitation was measured and the entire measurement setup was synchronized with the reference multisine signal. The current as well as the voltage impedance responses were passed through anti-Alias filters (1 MHz cutoff frequency) before the signals were sampled with the PXIe-5122, such that aliasing was also avoided.

Once the sampled noisy voltage and current observations were available to be processed, the impedance spectrum was computed using Matlab [15]. The signal linear time-invariant signal processing tool used to estimate the impedance was based on the short time Fourier transform (STFT) using overlapping records. The spectral leakage was intentionally avoided by setting the STFT window duration (i) by processing an integer number of periods of the reference for each record and (ii) by using a rectangular time sliding window.

A consistent impedance spectrum estimator $\hat{Z}(\omega_k)$ (when $P \rightarrow \infty$) is obtained in 1 by means of the division of the voltage-current sample mean Fourier coefficients at the excited frequencies [12], namely

$$\hat{Z}(\omega_k) = \frac{\hat{V}(k)}{\hat{I}(k)} = \frac{\frac{1}{P} \sum_{p=1}^P V^{[p]}(k)}{\frac{1}{P} \sum_{p=1}^P I^{[p]}(k)}, \quad (1)$$

with $\omega_k = 2\pi \frac{k}{T_{\text{ms}}}$, $\{V^{[p]}, I^{[p]}\}$ the excited discrete Fourier transform (DFT) bins of the p -th period of the current-voltage

signals. The impedance spectrum variance $\hat{Z}(\omega_k)$ was also quantified according to (2 [9]) at the excited frequencies. For further details on the signal processing, the reader is referred to [12].

Ultimately, the impedance was calibrated by measuring a reference resistor (199 Ω , 1%). The calibration experiment was carried out at the same measurement frequencies using the same measurement setup, such that the effects of the cables and the amplifier response on the measurement error were compensated.

For processing the data with the STFT-based technique, we chose a 10 ms window duration ($T_w = 10$ ms), such that it contained $N_{\text{ms}} = T_{\text{ms}}T_s = 5000$ samples per period. A total of $P_{\text{ms}} = T_w T_{\text{ms}} = 10$ multisine periods fitted in each block/segment, such that the number of samples within T_w was $N_w = P_{\text{ms}}N_{\text{ms}} = 5 \times 10^4$ samples. The measurement lasted for $T = 1$ seconds, giving a total of $N = T f_s = 5 \times 10^6$ samples the length of the voltage and current signals. Furthermore, the selected fraction of overlap (O) between segments was set to 60%, such that $O = 0.6N_w = 3 \times 10^4$ overlapping samples were used. In all, a total of 248 impedance spectra (26 frequencies) were processed in the 0.988 s recording period.

IV. EXPERIMENTAL RESULTS AND DISCUSSION

Figure 3 shows an example of the reactance spectra measured in the same muscle first relaxed and then contracted. Apart from the obvious difference between absolute values, there is no information available on how the impedance changed at the initiation of contraction.

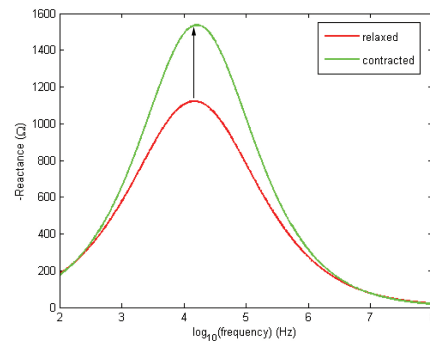


Fig. 3. Reactance spectrum measured in the relaxed (red) and contracted gastrocnemius (green). The arrow denotes the temporal change from one state to the other.

The temporal evolution of the contraction across the full range of frequencies measured is shown in Figure 4. As can be seen, the actual change in impedance during contraction is only a small fraction of the entire muscle impedance, speaking to the fact that muscle structure and integrity is

only minimally altered during the contractile process, despite the contractions being isokinetic and allowing for change in shape (as compared to isometric, where shape would remain for the most part unchanged). The reader is referred to [16] for further details on the results.

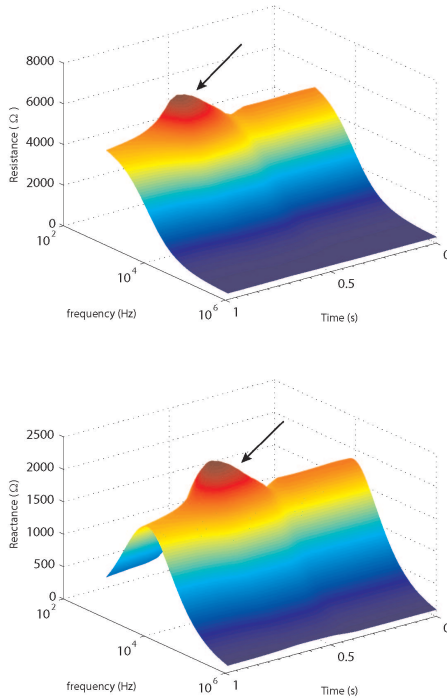


Fig. 4. Time-frequency dependence of resistance (top) and reactance (bottom) during contraction ($n=1$). The change in the resistance and reactance figures denoted by the arrows indicate the onset of the muscle contraction.

V. CONCLUSIONS

In this work, we apply the multisine electrical impedance myography (EIM) technique to study the bioimpedance spectroscopic features in a healthy mouse during electrical stimulation of the sciatic nerve. The impedance alterations are closely tied to the development of force and we identified changes in the impedance of the tissue post-contraction as compared to pre-contraction, possibly representing some fundamental alteration in the material properties of the muscle after contraction.

Dynamic EIM has the prospect of revealing new insights into the basic mechanical aspects of muscle behavior during active muscle contraction. Future work will be focused on measuring both the length and force with a dual-mode muscle lever system (Aurora Scientific, Aurora, Ontario, CA) synchronously to the impedance using our custom frequency response analyzer.

REFERENCES

[1] A. Ropper and M. Samuels, *Adams and Victor's principles of neurology*. New York: McGraw-Hill Professional, 2009.

[2] S. Cirak, L. Feng, K. Anthony, V. Arechavala-Gomez, S. Torelli, C. Sewry, J. E. Morgan, and F. Muntoni, "Restoration of the dystrophin-associated glycoprotein complex after exon skipping therapy in duchenne muscular dystrophy," *Molecular therapy : the journal of the American Society of Gene Therapy*, vol. 20, no. 2, pp. 462–7, 2012.

[3] S. Rutkove, "Electrical impedance myography as a biomarker for als," *Lancet Neurol*, vol. 8, no. 3, p. 226; author reply 227, 2009, 1474–4422.

[4] S. B. Rutkove, H. Zhang, D. A. Schoenfeld, E. M. Raynor, J. M. Shefner, M. E. Cudkowicz, A. B. Chin, R. Aaron, and C. A. Shiffman, "Electrical impedance myography to assess outcome in amyotrophic lateral sclerosis clinical trials," *Clin Neurophysiol*, vol. 118, no. 11, pp. 2413–8, 2007, 1388-2457.

[5] S. B. Rutkove, J. B. Caress, M. S. Cartwright, T. M. Burns, J. Warder, W. S. David, N. Goyal, N. J. Maragakis, L. Clawson, M. Benatar, S. Usher, K. R. Sharma, S. Gautam, P. Narayanaswami, E. M. Raynor, M. L. Watson, and J. M. Shefner, "Electrical impedance myography as a biomarker to assess als progression," *Amyotrophic Lateral Sclerosis*, 2012.

[6] C. A. Shiffman, R. Aaron, and S. B. Rutkove, "Electrical impedance of muscle during isometric contraction," *Physiol Meas*, vol. 24, no. 1, pp. 213–34, 2003.

[7] B. Sanchez, A. Aroul, E. Bartolome, K. Soundarapandian, and R. Bragos, "Propagation of measurement errors through body composition equations for body impedance analysis," *IEEE Transactions on Instrumentation and Measurement*, vol. 63, no. 6, pp. 1535–1544, June 2014.

[8] B. Sanchez, X. Fernandez, S. Reig, and R. Bragos, "An fpga-based frequency response analyzer for multisine and stepped sine measurements on stationary and time-varying impedance," *Measurement Science and Technology*, vol. 25, no. 1, p. 015501, 2014.

[9] R. Pintelon and J. Schoukens, *System identification: a frequency domain approach*, 2nd ed. IEEE Press, 2012.

[10] B. Sanchez, G. Vandersteen, R. Bragos, J. Schoukens, and C. R. Rojas, "On the calculation of the D-optimal multisine excitation power spectrum for broadband impedance spectroscopy measurements," *Measurement Science and Technology*, vol. 23, no. 23, p. 085702, Oct. 2012.

[11] B. Sanchez, E. Louarroudi, E. Jorge, J. Cinca, R. Bragos, and R. Pintelon, "A new measuring and identification approach for time-varying bioimpedance using multisine electrical impedance spectroscopy," *Physiological measurement*, vol. 34, no. 3, pp. 339–57, Mar. 2013.

[12] B. Sanchez, E. Louarroudi, R. Bragos, and R. Pintelon, "Harmonic impedance spectra identification from time-varying bioimpedance: theory and validation," *Physiological measurement*, vol. 34, no. 10, pp. 1217–1238, Sep. 2013.

[13] C. H. Hakim, N. B. Wasala, and D. Duan, "Evaluation of muscle function of the extensor digitorum longus muscle ex vivo and tibialis anterior muscle in situ in mice," *Journal of visualized experiments : JoVE*, no. 72, 2013.

[14] J. M. Shefner, A. G. Reaume, D. G. Flood, R. W. Scott, N. W. Kowall, R. J. Ferrante, D. F. Siwek, M. Upton-Rice, and J. Brown, R. H., "Mice lacking cytosolic copper/zinc superoxide dismutase display a distinctive motor axonopathy," *Neurology*, vol. 53, no. 6, pp. 1239–46, 1999.

[15] MATLAB, version 8.0.0.783 (R2012b). Natick, Massachusetts: The MathWorks Inc., 2012.

[16] B. Sanchez, J. Li, T. Geisbush, R. Bragos, and S. Rutkove, "Impedance alterations in healthy and diseased mice during electrically-induced muscle contraction," *IEEE transactions on bio-medical engineering*, vol. PP, no. 99, p. 1, Apr. 2014.